

流動床 내에서 固體粒子的 混合特性

李 源 國

韓 國 科 學 院

(접수 1975. 3. 14)

Mixing Behavior of Solid Particles in Fluidized Beds

Won Kook Lee

Korea Advanced Institute of Science, Seoul 131, Korea

(Received March 14, 1975)

要 約

流動床에서의 作動條件에 따른 固體粒子的 混合現象을 觀察하였으며, 現象의 直接觀察을 容易하게 하기 爲해 서 二次元床의 裏面の 光源이 床을 通過하는 光強度를 利用하였다. 그 結果 effective diffusivity는 大略 nh^2 에 比例하였으며, 또 diffusion parameter, \mathcal{D}_z/nh^2 , 는 system parameter, $\rho_p D_p/L\rho_f$, 및 operation parameter, $(U_0 - U_{mf})/U_{mf}$, 와 다음과 같은 關係가 있음을 알았다. 卽

$$\frac{\mathcal{D}_z}{nh^2} = 3.1 \times 10^4 \left(\frac{\rho_p D_p}{L\rho_f} \right)^{1.5} \left(\frac{U_0 - U_{mf}}{U_{mf}} \right)^{1.9}$$

Abstract

Phenomenon of solid-particle mixing in bubbling beds was observed with various operating conditions. Direct observation was easily achieved by using light intensity method through two-dimensional bed. The effective diffusivity was approximately proportional to nh^2 , and the diffusion parameter, \mathcal{D}_z/nh^2 , was correlated to the system parameter, $\rho_p D_p/L\rho_f$, and operation parameter, $(U_0 - U_{mf})/U_{mf}$, as

$$\frac{\mathcal{D}_z}{nh^2} = 3.1 \times 10^4 \left(\frac{\rho_p D_p}{L\rho_f} \right)^{1.5} \left(\frac{U_0 - U_{mf}}{U_{mf}} \right)^{1.9}$$

Introduction

The behavior of solid particles in the emulsion

phase of bubbling beds have been studied by a number of scientists. Several approaches have been used to study the rapid movement and mixing of solid particles in their experimental methods.^{1,3,7,10)}

Among these approaches, the random diffusion model of the solid particles is well recognized to describe the mixing phenomenon in the beds. And the random mixing is mainly caused by bubble motions in the bed. Kunii and Levenspiel⁵⁾ developed the diffusion model to their bubbling bed model by using interrelation between bubble motion and solid mixing, and Haines and King²⁾ have described this relation by their stochastic process approach.

Lee⁶⁾ observed the bubble-population distribution with bed height. Park et. al⁹⁾ investigated the properties of bubbles in fluidized bed by using their electro-resistivity probe. Haines and King²⁾ correlated the bubble motion to solid mixing. They concluded that the effective diffusion coefficient of solid particle mixing in the vertical direction by

$$D_z = D_{z0} + n/\beta^2 \quad (1)$$

and also they suggested that

$$\beta = 1/D_b$$

But none of the findings was observation of mixing behavior directly from the bed, and also there is no simple correlation directly usable for design of practical beds.

In this paper it is attempted to investigate the solid-particle mixing-behavior in tow-dimensional air-fluidized bed by observing direct way from the bed. The observations were made by light beam passing through the bed, and the intensities were checked. The solid particles used in this experiment were two types, tagged and untagged. Therefore, the light intensities passing through the bed were directly proportional to the mixing degree of the tagged particles at the point where light was passed. It is also tried to find a simple correlation between diffusivity and operating conditions in the bed.

Theoretical Consideration

Solid-particle mixing, according to the diffusion model, can be described by the diffusion equation

$$\frac{\partial C}{\partial t} = D \frac{\partial^2 C}{\partial Y^2} \quad (3)$$

with appropriate boundary conditions. For a vertical movement, the equation can be rewritten in the form

$$\frac{\partial C}{\partial t} = D_z \frac{\partial^2 C}{\partial Y^2} \quad (4)$$

The particle mixing coefficient, D_z , can be determined in large scale tests by means of black-tagged particles. The tagged particle were placed at the top of the fluidized bed and the appearance of black particles at various locations and time were traced by light beam through the bed.

The boundary conditions under these situations:

$$\text{at } t=0, C=C_0 \text{ for } 0 \leq Y \leq Y_1$$

$$C=0 \text{ for } Y_1 < Y \leq L$$

$$t=\infty, C=C_\infty = \frac{C_0 Y_1}{L}$$

$$\text{for } t > 0, \frac{\partial C}{\partial Y} = 0 \quad \text{at } Y=0 \\ Y=L$$

The solution of Equation (4) in the limit as Y_1 approaches to zero is⁷⁾

$$\frac{C}{C_\infty} = 1 + 2 \sum_{n=1}^{\infty} e^{-\left(\frac{n\pi}{L}\right)^2 \frac{D_z t}{L^2}} \cos \frac{n\pi Y}{L} \quad (5)$$

By comparing experimental data with calculations from Equation (5), it is possible to find the dispersion coefficient, D_z . Computer calculation of C vs. t and C vs. Y/L were plotted in Figs. 1 and 2, respectively.

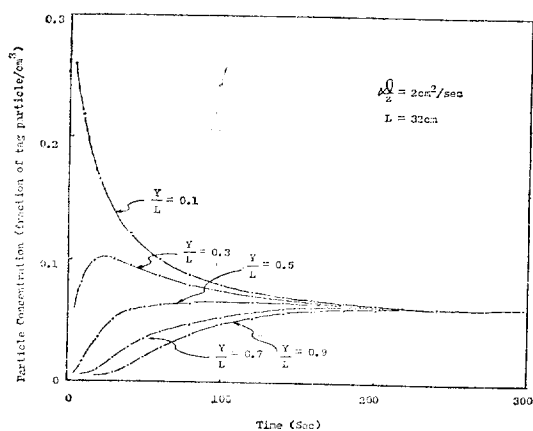


Fig. 1. Relation between particle concentration and time ($D_z = \text{constant}$)

Van Deemter¹¹⁾ expressed the axial dispersion coefficient of solid particles by interchange coefficient in

$$D_z = \frac{\left(\frac{\text{fraction of bed consisting of solid moving up-wards}}{\text{linear velocity of up-ward moving solids}} \right) \left(\frac{\text{interchange coefficient for solids, based on unit volume of bed}}{\text{volume fraction of the bed consisting of solids}} \right)}$$

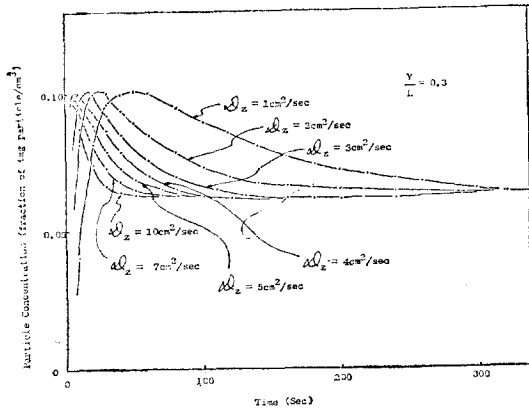


Fig. 2. Relation between particle concentration and time ($Y/L = \text{constant}$)

This expression can be rewritten in terms of the bubbling bed model³,

$$D_z = \frac{[\delta\alpha(1-\epsilon_{mf})]^2 (U_b)^2}{[\delta K] [(1-\delta)(1-\epsilon_{mf})]} \quad (7)$$

Where K is

$$K = \frac{3(1-\epsilon_{mf})}{(1-\delta)\epsilon_{mf}} \cdot \frac{U_{mf}}{D_b} \quad (8)$$

Combining Equations (7) and (8) gives

$$D_z = \frac{\alpha^2 \epsilon_{mf} \delta}{3U_{mf}} D_b U_b^2 \simeq \frac{\alpha^2 \epsilon_{mf}}{3\delta U_{mf}} D_b (U_0 - U_{mf})^2 \quad (9)$$

Theoretically this equation is interesting, but for practical purpose this gives difficulties and erroneous results because it has several factors such as α , ϵ_{mf} , δ , and these can not be evaluated in reasonable values either theoretically or experimentally. But Haines and King² proposed as

$$D_z = D_{z0} + nD_b^2 \quad (10)$$

Where D_b can be calculated from⁴)

$$D_b = 1.4\rho_p D_p (U_0/U_{mf}) \cdot h \quad (11)$$

As D_{z0} is the dense phase diffusion coefficient, the practical value is quite small compared with the bubbling bed diffusion coefficient, then

$$D_z \simeq nD_b^2 \\ = n[1.4\rho_p D_p (U_0/U_{mf}) h]^2 \quad (12)$$

Lee⁶) observed in his two-dimensional bed that

$$n/A = 220 \cdot e^{-0.12h} \quad (13)$$

Where n is in second, A is in ft^2 , and h is in inch. Combining Eqs(12) and (13) will give useful informations on diffusivity. But in this expression, the

height effect h on D_z is not so clear for practical usage in design purpose. Therefore, the efforts put in this experiment was aimed to find the simple relationship among D_z , $(U_0 - U_{mf})/U_{mf}$, and h .

By observation of Eqs. (9) and (12), it gives a certain suggestion that correlation can be shown in the following dimensionless form.

$$\frac{D_z}{nh^2} = \phi\left(\frac{D_p \rho_p}{L \rho_f}, \frac{U_0 - U_{mf}}{U_{mf}}\right) \quad (14)$$

Experimental Procedure

The bed (Fig. 3) was fluidized with compressed air through a pressure regulator. The pressure was regulated around 2kg/cm^2 . Glass beads (ranging from 40 to 100 mesh) were used for fluidized particles. Pressure and flow rate of inlet air were checked by a pressure gage and rotameter equipped on the inlet line. Tagged particles were coated with thin silver film by treating with silver nitrate solution and reduction agents, so that light beam cannot pass through tagged particles. The tagged particles were used in the bed with untagged glass beads, and particle-mixing was observed directly by light source from the opposite side of the bed. Figure 4 shows

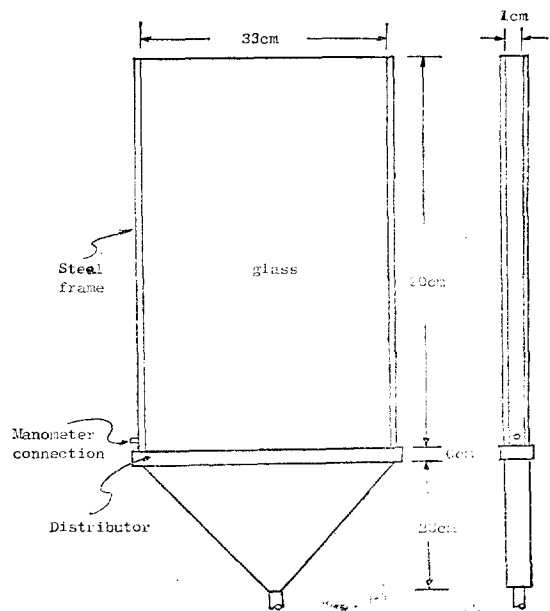
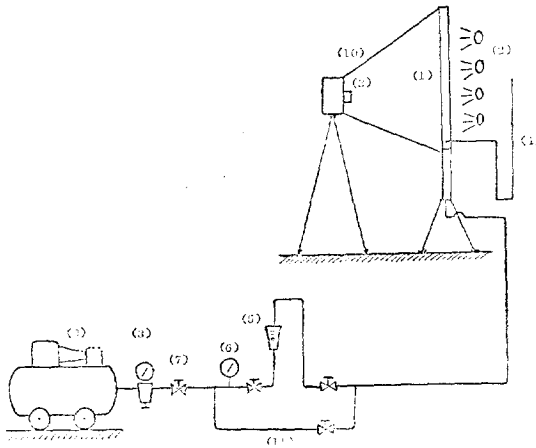


Fig. 3. Fluidized bed dimension



1. Bed
2. Light source
3. Camera
4. Manometer
5. Rotameter
6. Pressure gage
7. Needle valve
8. Pressure regulator
9. Air compressor
10. Light shield
11. By-pass Line

Fig. 4. Schematic arrangement of the experimental apparatus

the schematic diagram of the experimental apparatus.

The bed was fluidized for a given time intervals (10 to 30 seconds) and then stopped a while for taking pictures of the bed. As the light beams from the sources (4 of 500-watt flood bulb) were passed through the layer of glass beads, light intensities through the bed were exactly same proportion of the particles mixed with tagged particles. Therefore, the pictures by these light intensities showed the particle-mixing behavior caused by flow conditions in the bed.

The films were examined with a light intensity detecting system. The detecting device was consisted with a photocell, electric bulb, and multimeter, and the film was examined on the detecting device one at a time. Light intensities of various locations on the film were converted to particle concentrations by comparing with reference intensities. The reference intensities were obtained from the portions of tagged

and untagged particles in the pictures which were taken at initial stage of each run.

Pressure drops through the bed were measured by a monometer connected at the bottom of the bed. The minimum fluidization velocities in the bed were determined with the observation of the pressure drops.

Results and Discussion

Minimum fluidization velocities of the bed were determined by reading a break point in Fig. 5. The fluidized characteristics and operating conditions were tabulated in Table 1.

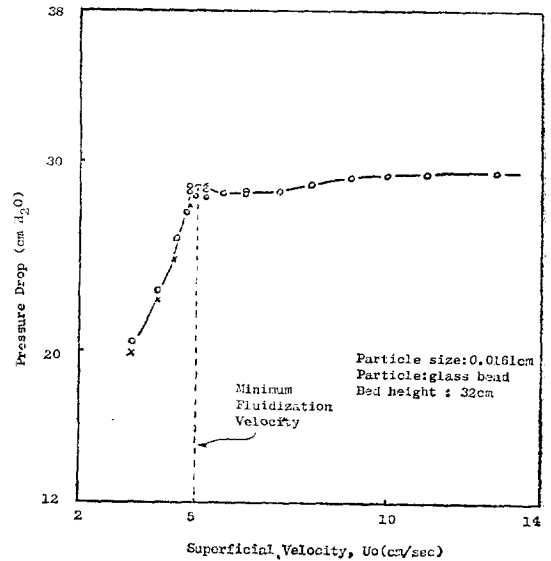


Fig. 5. Relation between pressure difference and gas superficial velocity

Table 1. Experimental data

U_0 (cm/sec)	U_{mf} (cm/sec)	D_p (cm)	h (cm)	n/A^* (no/sec-cm ²)	\bar{Q}_s (cm ² /sec)
11.75	5.0	0.0161	10	4.87	2.7
			16	3.67	5.1
			22	2.76	6.5
13.67	5.0	0.0161	10	4.87	4.2
			16	3.67	7.5
			22	2.76	10.5

9.00	5.0	0.0161	10	4.87	1.3
			16	3.67	2.0
			22	2.76	2.6
15.10	6.2	0.0212	10	4.87	4.2
			16	3.67	8.0
			22	2.76	10.0
13.20	6.2	0.0212	10	4.87	2.3
			16	3.67	4.0
			22	2.76	6.5
10.70	6.2	0.0212	10	4.87	1.2
			16	3.67	2.0
			22	2.76	3.0
19.30	11.2	0.030	10	4.87	1.7
			16	3.67	1.5
			22	2.76	5.0
17.70	11.2	0.030	10	4.87	1.0
			16	3.67	0.8
			22	2.76	2.4

*Calculated from Eq. (13).

Effective diffusivities, \mathcal{D}_z , of the particles were determined by comparing the observed data from the films and theoretical calculation of Eq. (5) or Fig. 2.

The bubble frequencies for a given bed height, n were calculated from Eq. (13). The correlations between bed height and effective diffusivity were plotted in Fig. 6 for given particle sizes. The results showed that \mathcal{D}_z were approximately proportional to nh^2 . This gives some confidence of Eq. (14).

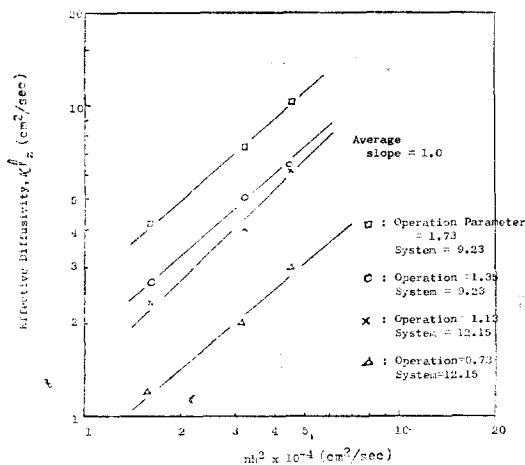


Fig. 6. Relation between effective diffusivity and nh^2

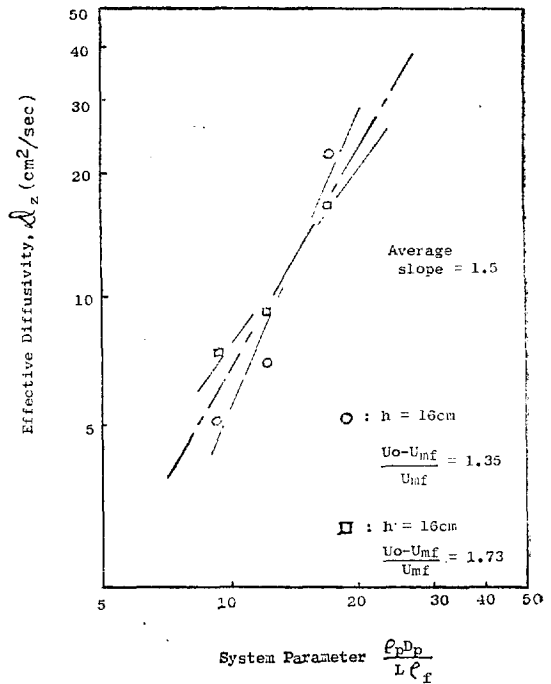


Fig. 7. Relation between effective diffusivity and system parameter

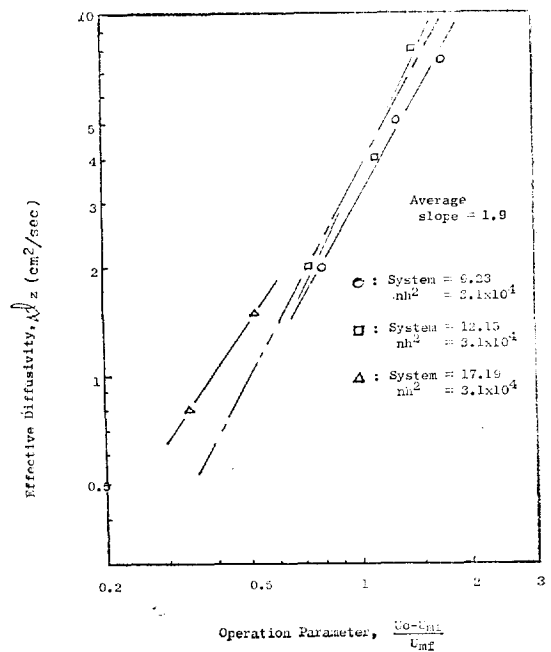


Fig. 8. Relation between effective diffusivity and operation parameter.

Correlation among dimensionless groups \mathcal{D}_z/nh^2 (diffusion parameter), $\rho_p D_p/\rho_f L$ (system parameter), and $(U_0 - U_{mf})/U_{mf}$ (operation parameter) were plotted in Fig. 7. and 8. These results showed that the diffusion parameter is proportional to $(D_p \rho_p / L \rho_f)^{1.5}$ and to $(U_0 - U_{mf})/U_{mf}^{1.9}$. All of the above results suggest an empirical formula of the form

$$\frac{\mathcal{D}_z}{nh^2} = B \left(\frac{D_p \rho_p}{L \rho_f} \right)^{1.5} \left(\frac{U_0 - U_{mf}}{U_{mf}} \right)^{1.9}$$

Figure 9 shows this correlation and the plotting gives the value B as 3.1×10^4 . Hence,

$$\frac{\mathcal{D}_z}{nh^2} = 3.1 \times 10^4 \left(\frac{D_p \rho_p}{L \rho_f} \right)^{1.5} \left(\frac{U_0 - U_{mf}}{U_{mf}} \right)^{1.9}$$

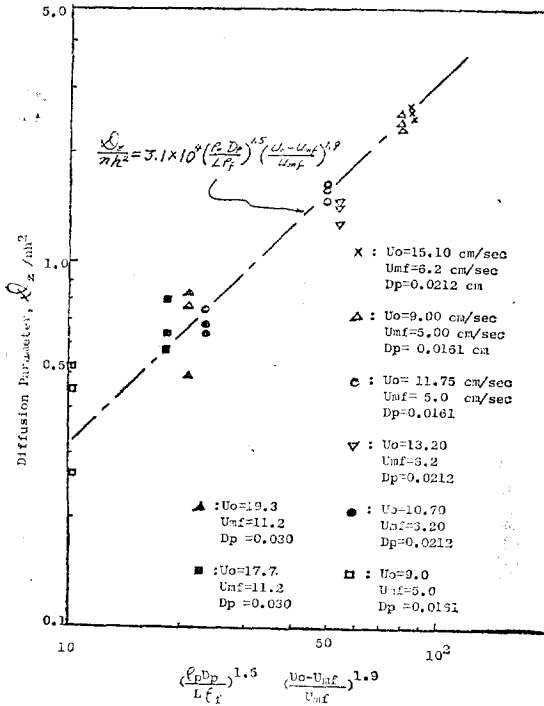


Fig. 9. Relation between diffusion parameter and operating conditions.

With this empirical equation, it is very easy to find the effective diffusivity by using system parameter from equipment, and operating parameter by operating conditions of any fluidized bed in mind.

Conclusions

1. Particle-mixing in a fluidized bed can be effectively

observed by the light intensity method.

2. Effective diffusivity varies with bed height, and approximately proportional to nh^2 .
3. The useful parameters in solid-particle mixing in fluidized beds are diffusion parameter $\left(\frac{\mathcal{D}_z}{nh^2}\right)$, system parameter $\left(\frac{\rho_p D_p}{L \rho_f}\right)$, and operation parameter $\left(\frac{U_0 - U_{mf}}{U_{mf}}\right)$ and these are correlated as
$$\frac{\mathcal{D}_z}{nh^2} = 3.1 \times 10^4 \left(\frac{\rho_p D_p}{L \rho_f} \right)^{1.5} \left(\frac{U_0 - U_{mf}}{U_{mf}} \right)^{1.9}$$

Nomenclature

- A Cross-sectional area of bed, cm^2
 B Constant, dimensionless
 C Concentration, fraction of tag particle/ cm^3
 D Diameter, cm
 \mathcal{D} Effective diffusivity, cm^2/sec
 h Bed height from the distributor, cm
 K Defined by Eq. (18)
 L Packed height of bed, cm
 n Bubble frequency, cm^{-1}
 t Time, sec
 U Flow velocity, cm/sec
 Y Bed height from top $= (L - h)$, cm
 Y_1 Height of tagged particle, cm
Greek letters
 α Ratio of wake volume to bubble volume, dimensionless
 β Jump parameter, cm^{-1}
 δ Fraction of fluidized bed consisting of bubbles, dimensionless
 ϵ Void fraction, dimensionless
 ρ Density, g/cm^3
Subscription
 b Bubble
 f Fluid
 p Particle
 mf Minimum fluidization
 o Operating
 z Axial-direction

References

1. M. M. El Halwagi and A. Gomezplata, *A. I. Ch.*

- E. Journal*, **13**(1967), 503.
2. A.K. Haines and R.P. King, *A.I. Ch. E. Journal*, **18**(1972), 591.
3. T. Hayakama, W. Graham and C.L. Osberg, *Canadian J. Chem. Eng.* **42**(1974), 99.
4. H. Kobayashi, F. Arai and T. Shiba, *Kagaku Kogaku (Japan)* **29**(1965), 858.
5. D. Kunii, K. Yoshida and O. Levenspiel, *I. & E.C. Fundamentals*, **8**(1969), 402.
6. W.K. Lee, "Bubble Behaviours in Air-Fluidized Beds", M.S. Thesis, University of Idaho, 1968.
7. W.G. May, *Chem. Eng. Progr.* **55**(1959), 49.
8. S. Morooka, Y. Kato and T. Miyauchi, *J. Chem. Eng. Japan*, **5**(1972), 63.
9. W.H. Park, W.K. Kang, C.E. Capes and G.L. Osberg, *Chem. Engng Sci.*, **24**(1969), 851.
10. P.N. Rowe and K.S. Sutherland, *Trans, Inst. Chem. Eng.* **42**(1964), T157.
11. J.J. Van Deemter, *Proc. Intern. Symp. on Fluidization*, Netherlands University Press, Amsterdam, 1967.

